



Mass data processing of time series Landsat imagery: pixels to data products for forest monitoring

Txomin Hermosilla, Michael A. Wulder, Joanne C. White, Nicholas C. Coops, Geordie W. Hobart & Lorraine B. Campbell

To cite this article: Txomin Hermosilla, Michael A. Wulder, Joanne C. White, Nicholas C. Coops, Geordie W. Hobart & Lorraine B. Campbell (2016) Mass data processing of time series Landsat imagery: pixels to data products for forest monitoring, International Journal of Digital Earth, 9:11, 1035-1054, DOI: [10.1080/17538947.2016.1187673](https://doi.org/10.1080/17538947.2016.1187673)

To link to this article: <https://doi.org/10.1080/17538947.2016.1187673>



© 2016 Her Majesty the Queen in Right of Canada. Published by Informa UK Limited, trading as Taylor & Francis Group



Published online: 13 Jun 2016.



Submit your article to this journal [↗](#)



Article views: 9977



View related articles [↗](#)



View Crossmark data [↗](#)



Citing articles: 66 View citing articles [↗](#)

Mass data processing of time series Landsat imagery: pixels to data products for forest monitoring

Txomin Hermosilla^a, Michael A. Wulder^b , Joanne C. White^b , Nicholas C. Coops^a, Geordie W. Hobart^b and Lorraine B. Campbell^a

^aIntegrated Remote Sensing Studio, Department of Forest Resources Management, University of British Columbia, Vancouver, BC, Canada; ^bCanadian Forest Service (Pacific Forestry Centre), Natural Resources Canada, Victoria, BC, Canada

ABSTRACT

Free and open access to the Landsat archive has enabled the implementation of national and global terrestrial monitoring projects. Herein, we summarize a project characterizing the change history of Canada's forested ecosystems with a time series of data representing 1984–2012. Using the Composite2Change approach, we applied spectral trend analysis to annual best-available-pixel (BAP) surface reflectance image composites produced from Landsat TM and ETM+ imagery. A total of 73,544 images were used to produce 29 annual image composites, generating ~400 TB of interim data products and resulting in ~25 TB of annual gap-free reflectance composites and change products. On average, 10% of pixels in the annual BAP composites were missing data, with 86% of pixels having data gaps in two consecutive years or fewer. Change detection overall accuracy was 89%. Change attribution overall accuracy was 92%, with higher accuracy for stand-replacing wildfire and harvest. Changes were assigned to the correct year with an accuracy of 89%. Outcomes of this project provide baseline information and nationally consistent data source to quantify and characterize changes in forested ecosystems. The methods applied and lessons learned build confidence in the products generated and empower others to develop or refine similar satellite-based monitoring projects.

ARTICLE HISTORY

Received 18 January 2016
Accepted 4 May 2016

KEYWORDS

Remote sensing; big data; forest; change; monitoring; image processing

1. Introduction

Information on land cover change and dynamics is required to support monitoring and reporting programmes as well as scientific objectives (Rogan and Chen 2004; Wulder, Kurz, and Gillis 2004; Townshend et al. 2011). Over large areas and long time periods, remotely sensed data sets are ideally suited to quantitatively capture and portray conditions at a given point in time as well as how these conditions are changing through time (Kennedy et al. 2009; Banskota et al. 2014; Gómez, White, and Wulder 2016). For consistent and defensible results, the application of transparent and reproducible methods is critical. Following the opening of the United States Geological Survey (USGS) archive of Landsat imagery (Woodcock et al. 2008) users have been provided with high-

CONTACT Txomin Hermosilla  txomin.hermosilla@ubc.ca;  txominhermos@gmail.com Integrated Remote Sensing Studio, Department of Forest Resources Management, University of British Columbia, 2424 Main Mall, Vancouver, BC, Canada V6T 1Z4

© 2016 Her Majesty the Queen in Right of Canada. Published by Informa UK Limited, trading as Taylor & Francis Group. This is an Open Access article distributed under the terms of the Creative Commons Attribution-NonCommercial-NoDerivatives License (<http://creativecommons.org/licenses/by-nc-nd/4.0/>), which permits non-commercial re-use, distribution, and reproduction in any medium, provided the original work is properly cited, and is not altered, transformed, or built upon in any way.

quality analysis-ready imagery at a spatial resolution that is informative at the scale of human interactions with terrestrial ecosystems (Wulder and Coops 2014). As a result, the user community has been active in developing approaches to utilize this heretofore unavailable source of image data (Hansen and Loveland 2012; Wulder et al. 2012). Projects that previously would have only been approachable with lower spatial resolution data sets have now been implemented using Landsat imagery, including global products such as forest change (Hansen et al. 2013), forest tree cover (Townshend et al. 2012; Sexton et al. 2013), readily available coverage for land cover mapping (Roy et al. 2010; Kovalevskyy and Roy 2013), and supra-national (Griffiths, Kuemmerle, et al. 2013; Potapov et al. 2015; Ju and Masek 2016) or national (Goward et al. 2008; Cohen et al. 2016) monitoring activities. In Canada, the National Terrestrial Ecosystem Monitoring System (NTEMS) project (White et al. 2014) aims to characterize the recent history of Canada's forests using Landsat data. These diverse projects, facilitated by free and open access to Landsat data, demonstrate the current state-of-the-art in computing and image processing.

Of the large area mapping and change detection projects indicated above, each of the projects, while similar in some respects, also have differing methodological approaches determined to meet specific project information needs (e.g. temporal window, geographical extent, and attributes captured), as well as decisions based upon image availability. For instance, a project implemented over the continental USA will have image availability (both spatially and temporally) in excess of all other regions globally (Ju and Roy 2008). Thus, methods developed for the continental USA might not be applicable elsewhere. Based upon the history of the Landsat sensors' data collection objectives, on-board storage capacity, and downlink, the global distribution of image availability is variable (Wulder, White, et al. 2015). In the case of Canada, there is a long history of cooperation with the USGS. The Canada Centre for Remote Sensing has been active in receiving imagery since 1972 and the archive has over 600,000 images representing Canada (White and Wulder 2013). While this number is large, the distribution of the images varies in space and time, and contains observations with atmospheric interference such as clouds, haze, smoke, and related shadows.

Pixel-based image compositing is an approach that can be implemented to address possible shortcomings related to image availability, atmospheric interference, phenology, and sun angles (Griffiths, van der Linden, et al. 2013; White et al. 2014). The time series-based change mapping method presented in Hermosilla et al. (2015a), hereafter referred to as Composite2Change (C2C), utilizes best-available-pixel (BAP) composites of surface reflectance values generated from archival Landsat imagery (White et al. 2014). Depending on the availability of data, atmospheric effects present, and compositing rules (e.g. temporal window and distance to clouds), some locations may result in pixels with 'no data' due to lack of suitable observations meeting the specific compositing criteria. These 'no data' instances require a step to fill in data gaps with proxy surface reflectance values to enable a gap-free spectral coverage of the given region of interest. As a result, image composites can include both measured and estimated values (Zhu et al. 2015). These image composites are the basis for producing a database of annual change occurring over Canada's forested ecosystems from 1984 to 2012 (Hermosilla et al. 2015b), with information produced on the amount, type, and rates of disturbances present. Options and approaches for dealing with sub-optimal spatial or temporal coverage of archival Landsat data will be of relevance to many nations and regions based upon historic satellite tasking, collection, receiving, and archiving practices (Wulder, White, et al. 2015).

Herein we present an example of the data processing decisions and related outcomes for a large area, time series, image compositing, and trend characterization project. Our objective is to report outcomes of various stages of the NTEMS project, from image availability through to product outcomes. The described image composite data represent a spatially and temporally comprehensive, nationally consistent source of information that has the spatial (30 m) and temporal (annual) resolutions necessary to characterize natural and anthropogenic changes. We present the results of a national implementation of a pixel-based image compositing approach using Landsat surface reflectance data described in White et al. (2014), and the subsequent filling of data gaps with proxy values. In addition, the change detection approach described by Hermosilla et al. (2015a), and the

attribution of change events to a change type, following methods described in Hermosilla et al. (2015b), have been implemented nationally, and herein, we present and implement a national accuracy assessment protocol on the C2C outcomes. We provide full details on the nature of the input data in order to improve understanding of the data outputs, and address the big data challenges of developing, producing, and validating gap-free digital geographic data products from the Landsat archive. We report and enumerate on the particulars of image inputs, including data gaps, and related needs for proxy infill generation. We aim to provide insights regarding algorithm development using the Landsat archive to characterize large areas over time. We also aim to be transparent in the decisions made for data processing and to inform on how these decisions impacted the final products, aided by the accuracy assessment presented. By sharing this example, we endeavour to inform implementation of similar projects by other research groups or operationally focused mapping agencies.

2. Study area

The generation of gap-free, surface reflectance BAP image composites was undertaken for Canada, which has a total area of approximately 998.5 million ha. To characterize forest change, we used the ecozone stratification of Canada (Ecological Stratification Working Group 1995). While we generated BAP composites for the entire country, our change analysis focused on those ecozones dominated by forest ecosystems (Figure 1). In Canada there are 10 ecozones that are dominated by forests, which represent more than 650 million ha, or approximately 65% of the national area (Wulder et al. 2008). These forest-dominated ecozones are a mosaic of trees, shrubs, wetlands, and lakes, with lesser components of urban infrastructure, agricultural lands, and alpine areas, among others. Canada's National Forest Inventory reports that treed and other wooded land in Canada occupy 388.4 million ha (Canadian Forest Service 2013).

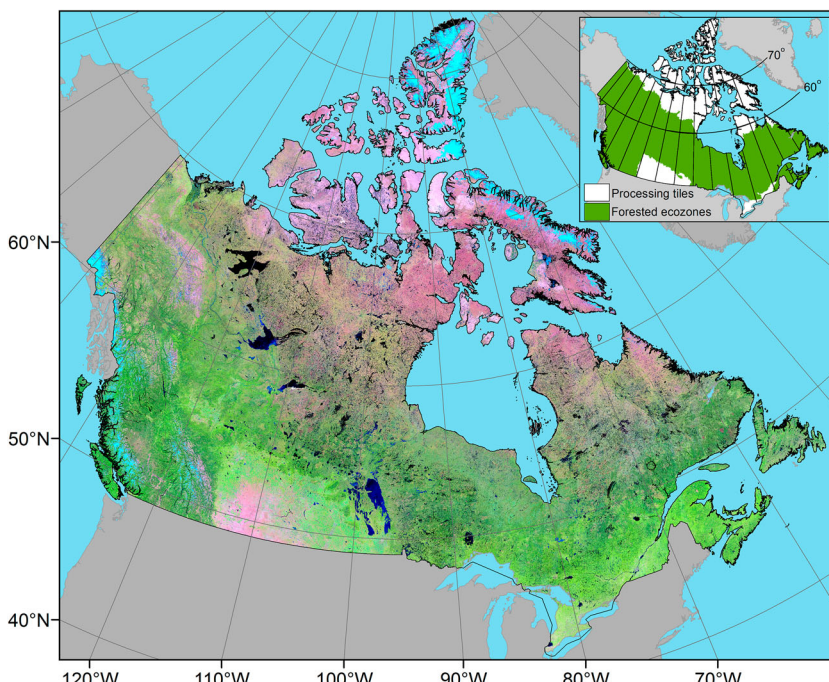


Figure 1. False colour (bands: 5–4–3) proxy image composite of Canada in 2000. UTM zones are partitioned into three latitudinal zones for data processing. In the map inset, ecozones dominated by forested ecosystems and the UTM processing zones are shown.

3. Data

The annual image composites were created by considering as candidate images all available Landsat Thematic Mapper (TM) and Enhanced Thematic Mapper Plus (ETM+) images (more than 81,000) from the 1285 scenes (path/rows) of the Landsat Worldwide Referencing System (WRS-2) in the USGS archive that covered at least part of the terrestrial area of Canada, had less than 70% cloud cover, and were acquired within a date range defined as 1 August \pm 30 days from 1984 to 2012. The date 1 August (Julian day 213) was designated as the central target acquisition date due to its correspondence with the growing season for the majority of Canada's terrestrial area (McKenney et al. 2006). All candidate images were downloaded from the archive as Level-1 Terrain-Corrected (L1T) products. Then we produced atmospherically corrected surface reflectance values for the six Landsat optical bands (bands 1–5, 7) using the Landsat Ecosystem Disturbance Adaptive Processing System (LEDAPS) algorithm (Masek et al. 2006; Schmidt et al. 2013). Clouds, related shadows, and other unwanted atmospheric elements are detected and masked using the Fmask algorithm (Zhu and Woodcock 2012). Note that this algorithm has been improved since our algorithm was developed and initially implemented, as described in Zhu and Woodcock (2014) by additionally considering the temporal information in the cloud detection. As the same water body can appear different both within and between years due to wind, ice, sedimentation, and changes in volume, among other factors, Fmask outputs were also used to define a water mask, which enabled the exclusion of water bodies from further analysis (Lunetta et al. 2004).

4. Methods

4.1 Processing tiles and data processing approach

To reduce resampling operations, we divided the country longitudinally into 17 processing tiles, corresponding to UTM zone boundaries (the L1T native projection), from UTM zone 7 to zone 22. Due to the northward narrowing of the UTM zones, the overlap between zones is about 30% at the southern border (e.g. 49° N) and up to 90% in the far north. Additionally, we divided each UTM zone into three latitudinal zones: South (southern border–60° N), North (60–70° N), and Arctic (70–83° N), see Figure 1. The temporal window for the image compositing approach was 1984–2012. The change analysis was performed in the period 1986–2010 and the two pairs of remaining years at the beginning (1984, 1985) and end (2011, 2012) of the time series were not mapped in the change analysis due to lack of pre- and post-event data. Also, since our analysis of change focused on the forested areas, we used a mask provided by Agriculture and Agri-Foods Canada (2011 data) to identify and exclude agricultural lands from our change characterization analyses.

Remote sensing big data computing is a challenging task due to the extensive nature of the analysis, combined with the large amount of data handled (Ma et al. 2015). In order to minimize time requirements and overcome memory issues, our methodologies were optimized to avoid processes requiring intensive RAM use, which permitted parallel processing at different sections of the processing tiles. Following this premise, we used the image line as basic processing unit, which required constant reading/writing data, being thus the input/output operations per second capabilities of the hard disk drives the only time limiting factor in our processing chain.

4.2 Overview of methods

The C2C methodology used to produce annual BAP image composites (White et al. 2014), infill data gaps caused by missing data and noise filtering, detect and characterize changes (Hermosilla et al. 2015a), and attribute detected changes (Hermosilla et al. 2015b) is detailed in the references indicated. A brief overview of the C2C methodology is provided below and presented in Figure 2.

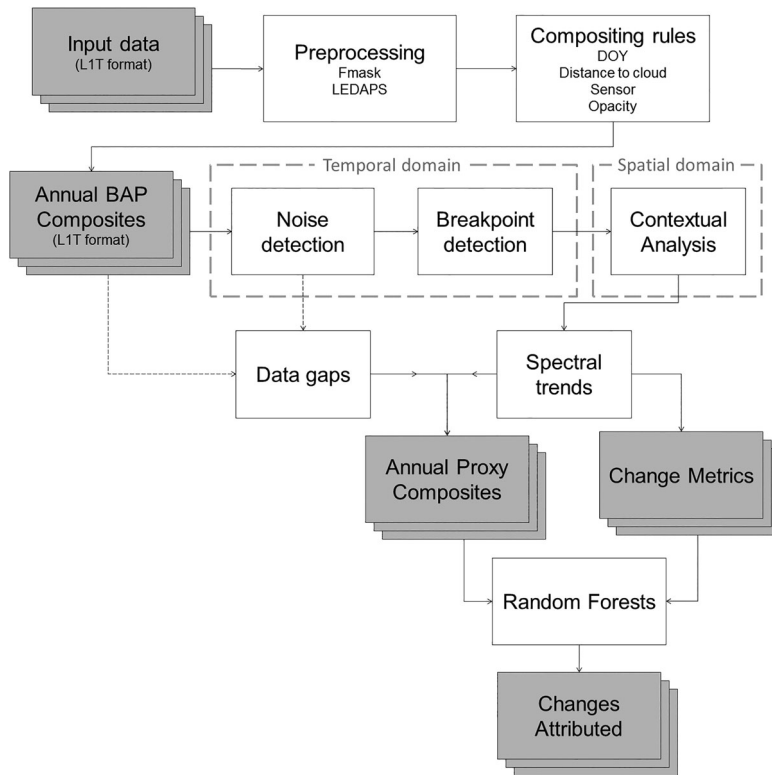


Figure 2. Overall workflow of the C2C methodology.

There are some instances where methods were improved from the originally published versions, prior to national implementation, and these instances are noted where appropriate.

Utilizing the consistently calibrated data record of the Landsat series of satellite (Markham and Helder 2012) we obtain and avail upon all candidate images to produce annual BAP image composites following the pixel-scoring functions described in White et al. (2014). These functions score each pixel observation for (i) sensor, (ii) acquisition day of year, (iii) distance to clouds and cloud shadows, and (iv) atmospheric opacity. Of note, we increased the penalty for ETM+ Scan Line Corrector (SLC)-off data from what was reported in White et al. (2014), changing the sensor score for ETM+ SLC-off (i.e. after 31 May 2003) from 0.5 to -0.7. This scoring ensured that TM data had preference over ETM+ post SLC-off, avoiding the use of multiple discontinuous small portions of images to produce the BAP image composites, thus reducing the spatial variability of the spectral data. A systematic operator-guided post-processing screening step was also applied using the temporal series of imagery to highlight locations, and remove offending images, where a geographic mismatch was present. As per White et al. (2014), the surface reflectance values of the pixel with the highest summation of the four scores was then used in the BAP image composites for a given year. Based on the compositing rules, 73,544 Landsat images contributed pixels to the 29 annual BAP composites. Those pixels without suitable observations are labelled as 'no data' and constitute data gaps that are addressed later in the C2C protocol.

Using values of the normalized burn ratio (NBR) (Key and Benson 2006) in the temporal domain (i.e. a vector of annual NBR values for each pixel), the C2C protocol (i) filters anomalous spectral observations resulting from unscreened cloud or cloud shadows, or by haze or smoke (similar to Kennedy, Yang, and Cohen 2010), removing those observations from the analysis (and hence producing more data gaps), and (ii) detects changes and temporal trends by applying the bottom-up

breakpoint detection algorithm proposed by Keogh et al. (2001) (see Figure 3). Since changes are detected from the spectral trajectories (i.e. temporal domain) they may result in spatially discordant events. Thus, a contextual analysis of the detected changes is then performed on the spatial domain to improve the consistency and spatial cohesion of the change features generated. This contextual analysis is undertaken in the spatial domain, and it is based on ranking the confidence in correctly defining a change in a given year. This confidence is inversely related to the amount of missing data before, during, and after the change event. Thus, detected changes with no or few instances of missing data are considered reliable and subsequently labelled with the change year. Changes with abundant missing observations are considered to have a lower reliability. Low reliability changes that were spatially adjacent to a high-reliability change within ± 1 year are re-labelled with the year of the more reliable spatially adjacent change, as detailed in Hermosilla et al. (2015a). Additionally, in this step we removed change events with an area smaller than the minimum mapping unit (MMU). The MMU size was determined to support the information needs of Canada National Forest Inventory (0.5 ha).

Data gaps resulting as a function of scoring criteria for BAP selection (hereafter referred as no-data observations) or as a function of subsequent noise filtering that is applied to the annual image composites, are infilled with proxy surface reflectance values. The infill value for a given pixel is determined using the spectral trends computed in the breakpoint detection process described above, which serves as a guide for a piecewise linear interpolation of the spectral values in that pixel's time series. This process results in gap-free, surface reflectance image composites at the native Landsat 30 m spatial resolution, which are hereafter referred to as proxy image composites. As an example, a proxy image composite for Canada for the year 2000 is shown in Figure 1.

From the spectral trend analysis (Figure 3) we also derive a set of descriptive change metrics that characterize forest change events, as well as pre- and post-change conditions (Table 1). These metrics allow for a distillation of the complex change trajectories and provide information that can be used to determine trends and support the labelling of change types. Note that in Hermosilla et al. (2015a), we recorded only the greatest change event, that is, the change event with the greatest magnitude in the time series. We subsequently altered the processing to capture multiple change events in the time series for each pixel and likewise generated additional metrics to characterize the first and last change events. Metrics are grouped into pre-change (Figure 3, segment AB), change (segment BC), and post-change (segment CD) categories. Change metrics characterize the negative trend segments according to the occurrence year, duration of the event, spectral difference before and after the change event (change magnitude), and change rate. Change rate is defined as the ratio of the change magnitude and the duration of that change process, and provides insights regarding the severity and speed with which changes occur. Pre- and post-change metrics inform about the spectral condition before and after the change event. Of special interest is the post-change evolution rate metric, which is

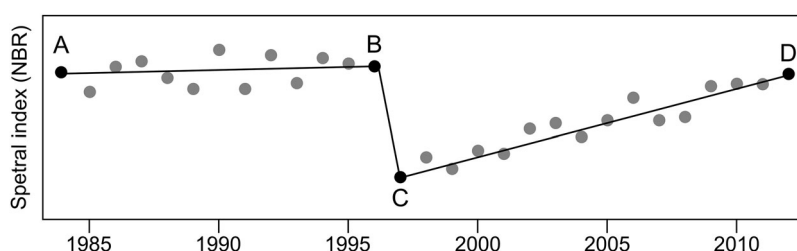


Figure 3. Graphical depiction of spectral trends and breakpoints used to calculate change metrics for a single pixel of Landsat time series data.

Table 1. List of spectral trend metrics generated to characterize change events. Nomenclature referred to Figure 3.

	Metric	Description
Pre-change ^a	Pre-change magnitude variation	Difference between NBR values at the start (A) and end (B) points of the pre-change segment
	Pre-change persistence	Number of years between the start (A) and end (B) points of the pre-change segment
	Pre-change evolution rate	Ratio of pre-change magnitude variation to pre-change persistence
Change (negative segments)	Change year	Year in which breakpoint occurs (C). For pixel series with multiple change events, this is the year in which the greatest change event occurs (greatest magnitude change). The breakpoint separates the pre-change and change segments
	Change persistence	Number of years between start (B) and end (C) points of the change segment
	Change magnitude variation	Difference between NBR values at the start (B) and end (C) points of the change segment
	Change rate	Ratio of change magnitude to persistence
	First change year	For pixel series with multiple change events, this is the year of the first change event (first breakpoint)
	First change persistence	For pixel series with multiple change events, this is the persistence of the first change event (first breakpoint)
	Last change year	For pixel series with multiple change events, this is the year of the last change event (last breakpoint)
	Last change persistence	For pixel series with multiple change events, this is the persistence of the last change event (last breakpoint)
	Post-change magnitude variation	Difference between NBR values at the start (C) and end (D) points of the post-change segment
Post-change ^a	Post-change persistence	Number of years with no negative segments years following a change event
	Post-change evolution rate	Ratio of post-change magnitude variation to post-change persistence

^aPre- and post-change metrics are calculated for the change event with the greatest magnitude in the pixel series.

related to the rate of spectral recovery following a change event. Values close to zero indicate very slow post-disturbance regrowth whereas higher values are associated with higher rates of vegetation return following disturbance, as described in Pickell et al. (2016) and Bartels et al. (2016).

Finally, following the object-based image analysis approach presented in Hermosilla et al. (2015b), the changes detected are attributed to a change type (fire, harvesting, road, or non-stand replacing). Non-stand-replacing change category refers to gradual changes in vegetation that do not lead to a change in land cover class (i.e. disease, insects, water stress, and decline). These changes are related to temporary variations (pulsed) in the vegetation condition (Vogelmann et al. 2016) or indicative of longer term directional alteration in vegetation condition apparent using time series (Cohen et al. 2016; Gómez, White, and Wulder 2011).

The change attribution is implemented at the object-level based on the spectral, temporal, and geometrical characteristics present using a random forests classifier (Breiman 2001). The spectral characteristics include average of the spectral values of the objects before the change event, average and standard deviation after the change event, and range, average and standard deviation of the values of the pixel series. These metrics are derived from the spectral bands 3, 4, 5, and 7, and for the indices NBR, and brightness, greenness, and wetness components from the Tasselled Cap (Crist 1985). The temporal metrics are computed from the spectral trend analysis, and provide information about the spectral response of change events as well as pre- and post-change conditions. Duration represents the time over which the event takes place. Magnitude variation is the difference between the average spectral values before and after the change event. Pre-change and post-change conditions are characterized by the magnitude variation, duration, and evolution rate (i.e. ratio between magnitude variation and duration). The geometry and shape complexity of a given change object is also described using area, perimeter, compactness, shape index, and fractal dimension. The number of votes received by each change class is used to define and act as an indicator of attribution confidence (Mitchell et al. 2008), in our approach computed as the ratio between the percentage of

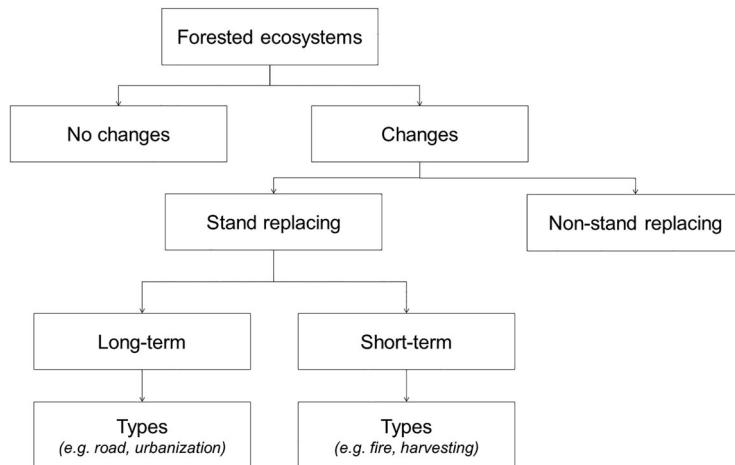


Figure 4. Forest change attribution hierarchy. Source: Adapted from Hermosilla et al. (2015b).

votes of the second most voted class and the percentage of votes of the attributed class. With this attribution confidence indicator, we prevent attributing objects to a change class when the confidence is very low (i.e. near even probability between two or more classes), labelling instead these change objects as unattributed. This will enable further interrogation and characterization of unclassified change objects based on additional metrics.

In Figure 5 we show a selection of the change products resulting from the application of the aforementioned methodologies. In Figure 5(a) we show the year in which the greatest change was detected, while Figure 5(b) presents the attribution of those change events into one of the four dominant change types. Additionally, metrics derived from the spectral trend analysis process are presented, including change rate (Figure 5(c)) and post-change evolution rate (Figure 5(d)). As an

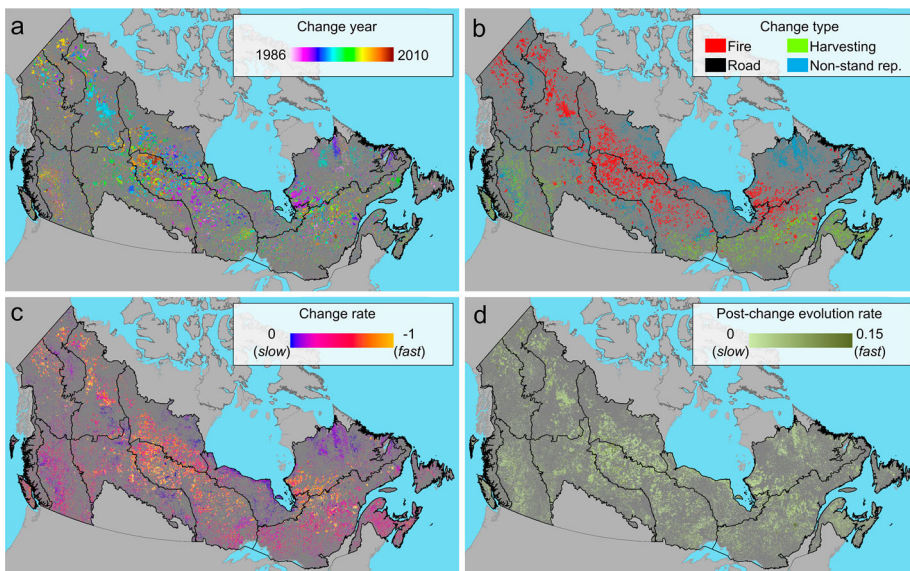


Figure 5. Forest change products derived from spectral trend analysis of annual Landsat composites: (a) changes labelled by detection year; (b) attribution of those changes into a forest change type; (c) change rate; and (d) post-change evolution rate metrics.

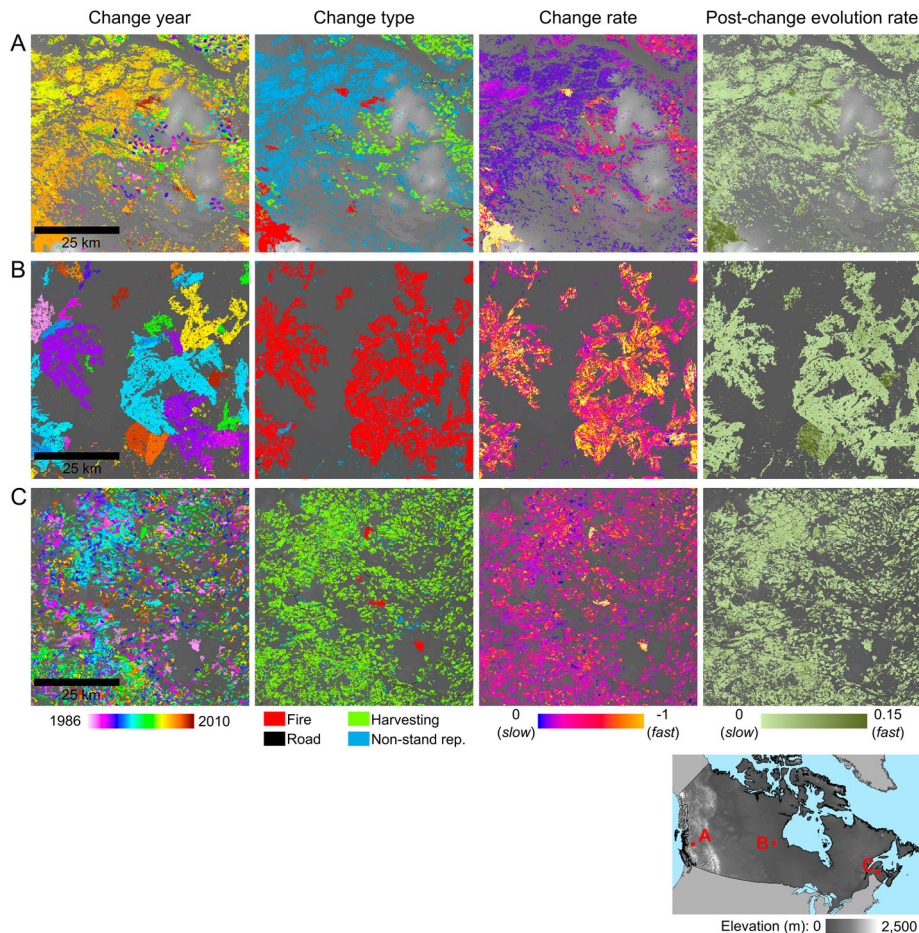


Figure 6. Examples of the forest change products derived from spectral trend analysis of annual Landsat composites in three different disturbance dominated ecozones: (a) Montane Cordillera, (b) Taiga Shield West, and (c) Atlantic Maritime.

integrating example, in Figure 6 we show detailed subsets of forest change detection year, change type attribution, and select change metrics in three locations dominated by different disturbance regimes, specifically the Montane Cordillera, Taiga Shield West, and Atlantic Maritime ecozones.

4.3 Assessment of forest change detection, date labelling, and attribution to change type

A stratified random sampling strategy was applied to select evaluation samples for the change detection and attribution processes following the approach described in Olofsson et al. (2014) and guided by Hermosilla et al. (2015b). At the highest level of our change hierarchy (Figure 4), we evaluated the efficacy of our change detection, allocating the total number of sample points ($n = 1200$) equally to our change and no change strata. We also evaluated our change attribution, whereby we assigned detected change events to one of four change types. The 600 samples within the change strata were allocated equally to the four change types ($n = 150$) (fire, harvest, road, and non-stand replacing). Finally, as we captured 25 years of change, we wanted to report the frequency with which change events were detected within the correct year. To this end, we also distributed the 600 samples equally among the 25 years; however, as the sample size for any given year is small, we do not report the accuracy of attribution by year. Each sample was manually interpreted by the same interpreter,

who was trained to visually recognize the four change types, and was given reference examples to use as a guide. Interpretations were vet by a second, independent interpreter to ensure consistency. The annual BAP images composites and high spatial resolution imagery from Google Earth™ were the main reference data sources. Additionally, other ancillary information were used to support interpretation, including the Canadian National Fire Database (Canadian Forest Service 2015) and regional spatial coverages depicting insects, and flagged as either change or no-change. In the case of change, the year and change type were also recorded.

The accuracy on the detection of changes was assessed using a confusion matrix based on estimated class area proportions, from which overall user's and producer's accuracies per class were computed to assess the commission and omission errors as well as error bounds (Olofsson et al. 2014). The temporal accuracy of the change detection was also evaluated by comparing the change year with the reference year. We assess the temporal accuracy of detected changes occurring within three years of the reference events. Changes detected with a difference of four or more years were directly flagged as detection errors. We likewise used a confusion matrix based on estimated class area proportions to evaluate the accuracy on the attribution of the change agent.

5. Results

5.1 Image composite assessment

As Figure 7 indicates, data gaps resulting from missing observations (no data) and noise filtering varied, as well as the number of Landsat images used annually to create the image composites. Three different periods can be observed: TM, TM and ETM+ combined, and ETM+. During the period where only TM data were available (1984–1998), an average of 1802 images ($\sigma = 245.9$) were used each year and 14.2% ($\sigma = 5.5\%$) of pixels, on average, had no valid observations (no data). Between 1999 and 2011, TM and ETM+ sensors were in simultaneous operation, which boosted the average number of images used to build the annual composites to 3420 ($\sigma = 439.2$). The proportion of pixels with no data reduced to 5.9% ($\sigma = 1.6\%$). The majority of the images used in the compositing process prior to the malfunction of the Landsat 7 SLC in May 2003 were acquired by ETM+ (68% annual average). This changed during the SLC-off mode, with ETM+ providing, on average, only the

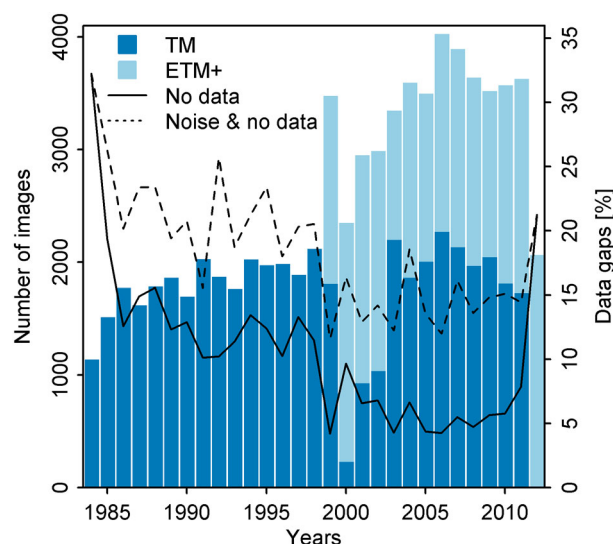


Figure 7. Number of images used annually in the image compositing process grouped by sensor, and percentage of data gaps due to the compositing (no data) and the noise detection processes.



44% of the images. Finally, when Landsat 5 TM operational imaging effectively ended after the 2011 northern hemisphere growing season (November 2011), only ETM+ acquisitions were available during 2012, which substantially reduced the number of used images to 2064 and resulted in an increase to 21.3% of no-data pixels in the compositing process due to the persistence of SLC-off data gaps. On average, the noise detection process applied to detect and remove noisy observations or anomalous values from the BAP image composites adds 8.4% ($\sigma = 2.4\%$) to the annual total data gaps.

The national spatial distribution of the number of years with data gaps is shown by Figure 8(a). Overall, a north/south striping across the entire country is evident and results from the satellite's polar orbit and related path overlap (which increases with latitude). Interior areas with flat topography are less prone to persistent cloud cover (i.e. Prairies, Boreal Plains, and Taiga Plains) and show more complete data while areas located east of Hudson Bay, and mountainous areas in the west, have a larger proportion of pixels with no data. Even with the high level of imaging overlap, the northern most islands of the Canadian Arctic Archipelago (i.e. Ellesmere Island and Axel Heiberg Island) are

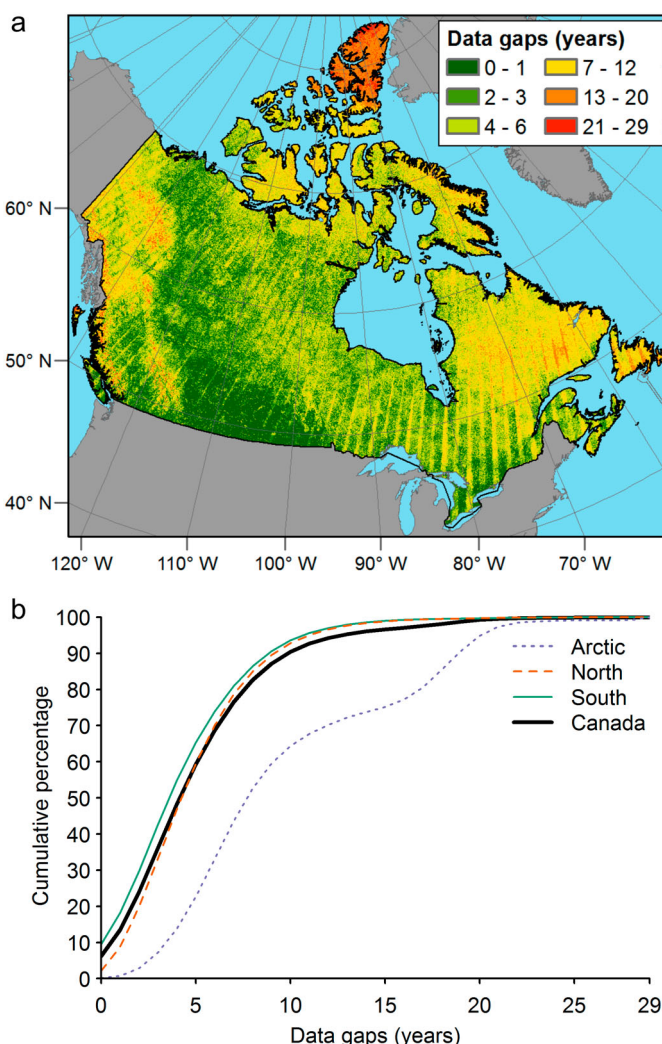


Figure 8. Spatial distribution of data gaps (a), and histogram of the cumulative percentage of data gaps (b) for Canada, and the three latitudinal zones defined: South, North, and Arctic.

found to be challenging locations to obtain valid observations due to the lower number of images acquired at these latitudes (based upon acquisition plans), combined with the persistent cloud cover that is common in these areas. Figure 8(b) shows the histograms with the cumulative percentage of data gaps: nationally, 59.2% of the observations have 5 data gaps or less; 90.4% of the pixels have 10 gaps or less; and 99.6% of observations had less than 22 years of missing data. Stratifying by latitudinal zones the South (southern border – 60° N) and North (60–70° N) display similar trends, with the Arctic (70–83° N) showing alternate trends. Given the forest focus of the NTEMS project, the characteristics in the South and North partitions identified here are of especial interest. When considering only these two regions, 63.3% of the observations have 5 data gaps or less; 93.3% of the pixels have 10 gaps or less; and 99.8% of observations had less than 22 years of missing data. In contrast, the Arctic zone (70–83° N) shows the largest proportion of data gaps, where 22.7% of the pixels have 5 gaps or less, 64.4% have 10 gaps or less, and 97.4% of pixels contained less than 22 years of missing data.

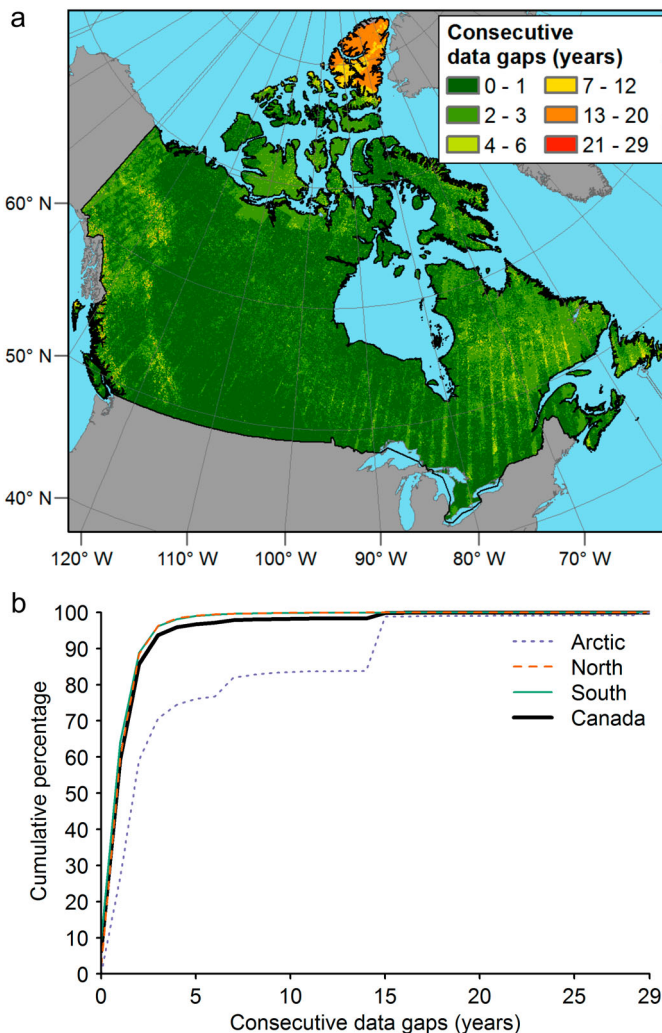


Figure 9. Spatial distribution of consecutive data gaps (a), and histogram of the cumulative percentage of consecutive data gaps (b) for Canada, and the three latitudinal zones defined: South, North, and Arctic.

When examining consecutive data gaps, we found that 59% of pixels had no persistent missing data (i.e. the number of consecutive data gaps or years of missing data was ≤ 1) ([Figure 9\(b\)](#)), 85.7% of the pixels had 2 consecutive gaps or fewer, and 99.8% of the pixels have 15 or fewer consecutive years of data gaps. As expected, the locations with a larger number of consecutive data gaps coincide spatially ([Figure 9\(a\)](#)) with a regional and/or satellite orbital explanation to the areas that have a larger proportion of data gaps in the time series. Within the Arctic zone consecutive data gaps are common, with a notable breakpoint evident between 14 and 15 years, passing from 83.8% to 98.8% of the observations, corresponding with a period prior to 1999, which had few acquisitions and persistent cloud coverage found for particular WRS-2 scenes.

5.2 Assessment of forest change detection and attribution

The confusion matrix of the change detection assessment by estimated proportions of area is shown in [Table 2](#). The overall detection accuracy is $0.89 (\pm 0.024)$. User's accuracies are high for both change (0.92 ± 0.02) and no change (0.88 ± 0.02) categories. The producer's accuracy is very high for no change class (0.98 ± 0.01) and significantly lower for change class (0.61 ± 0.04). The analysis of the change detection rate per class ([Table 3](#)) indicates that about 96% of samples allocated in both fire and harvesting categories are satisfactorily detected, and that road class has the lowest detection rates (66.3%). 89.3% of the changes are labelled to the correct year, and 97.7% are within ± 1 year. [Table 4](#) shows the change attribution assessment result, with an overall accuracy of $0.92 (\pm 0.024)$. Fire shows the highest user's accuracy (i.e. lowest commission error) and notable separability with the other identified stand-replacing and non-stand-replacing changes. The forest harvest class has balanced user's (0.88 ± 0.05) and producer's (0.88 ± 0.05) accuracies, with some confusion with roads, since these two events often occur simultaneously, in proximity, and have similar spectral characteristics resulting in the lowest producer's (0.36 ± 0.09) and user's (0.75 ± 0.07) accuracies for the road class.

6. Discussion

We have presented outcomes of the NTEMS project: a 30-m Canada-wide product based on time series of gap-free Landsat surface reflectance image composites for the characterization of forest changes and dynamics across three decades using the C2C protocol ([Hermosilla et al. 2015a](#)). This research has been made possible by free and open access to Landsat data ([Woodcock et al. 2008](#); [Wulder et al. 2012](#); [Wulder and Coops 2014](#)), new processing (e.g. [Griffiths, van der Linden, et al. 2013](#); [White et al. 2014](#)) and methodological opportunities ([Hansen and Loveland 2012](#)), as well as the richness of the Landsat archive over Canada ([White and Wulder 2013](#)), in contrast to many nations and regions globally ([Wulder, White, et al. 2015](#)).

This project represents an example of the new opportunities for information generation using remotely sensed data based upon access to large amounts of analysis-ready images ([Hansen and Loveland 2012](#); [Ma et al. 2015](#)). There are a growing number of examples for this type of large area, multi-temporal application with the particulars of the approach based upon the region of interest and/or the information need of the project ([Roy et al. 2010](#); [Townshend et al. 2012](#); [Hansen et al. 2013](#); [Potapov et al. 2015](#)). Pixel-based image compositing allows for terabytes (TB) of data to be

Table 2. Confusion matrix of estimated proportions of area for change detection assessment ($p < .05$).

	Reference					
	Change	No change	Total	User's accuracy	Producer's accuracy	Overall accuracy
Change	0.149	0.014	0.163	0.92 ± 0.02	0.61 ± 0.04	0.89 ± 0.025
No change	0.097	0.740	0.837	0.88 ± 0.02	0.98 ± 0.01	
Total	0.246	0.754	1.000			

Table 3. Detection rate per change class type.

Class	Detection rate
Fire	95.9%
Harvesting	96.2%
Non-stand replacing	83.5%
Road	66.3%

temporally and spatially considered in an automated fashion to extract selected pixels to ultimately produce detailed information about land cover and land cover change, among other outputs (Hansen and Loveland 2012; White et al. 2014).

To allow for consistency in image values over space and time, we converted all pixels to surface reflectance (with the LEDAPS algorithm; (Masek et al. 2006)). Implementing the Fmask algorithm (Zhu and Woodcock 2012) allowed for screening of undesired atmospheric effects and related artefacts (clouds, haze, through to shadows), to create masks, and produce scores to be used in pixel selection. With Canada at nearly 1 billion ha in size, at the 30 m Landsat spatial resolution the country is comprised of more than 10 billion pixels, with even more having been processed due to the methods applied and the overlap between UTM zones. To obtain an idea of the amount of data processed and storage requirements, one can multiply the number of pixels (10 billion) by the number of bands, number of years, processing masks (e.g. water, data availability, noise, snow), spectral trend analysis information, and bit depth (e.g. byte, integer, and float formats) of each spatial layer under consideration. For NTEMS, this results in over 400 TB of data to ultimately produce about 25 TB of Canada-wide seamless surface reflectance composites and time series land change information products. By way of elaboration, more drive space is required (~600 TB in our case) than complete data storage needs due to the nature of how the data is partitioned onto drives for processing (by UTM sub-zone processing tiles).

In support of our forest-focused application we had precise information of the location of the agricultural areas enabling exclusion of these highly variable (within and between year) from the change analysis. However, we do note that imagery from multiple seasons would enable additional information to aid in discrimination between forest and croplands, as well as for the labelling of land cover (e.g. Dymond et al. 2002). We produced phenologically consistent composites by restricting the image acquisition date to a 60-day window corresponding to the vegetation growing season in most Canadian forest ecosystems (i.e. July and August). This definition of the image acquisition range could be further refined by locally adapting the growing season dates based on latitude (Zhou et al. 2001). In restricting acquisition dates, we limit both phenological variation as well as the number of candidate observations, the latter of which increases the chance of data gaps that require to be filled with estimated surface reflectance values.

Overall, the amount of data gaps within Canada's forested ecosystems is limited, especially when compared with the non-forested Arctic latitudes, which have both a greater number of data gaps and a greater number of consecutive data gaps. Other regions (i.e. Pacific Range, Rocky Mountains, Labrador Peninsula, and Island of Newfoundland) are characterized by a greater number of data gaps,

Table 4. Confusion matrix populated by estimated proportions of area for forest change attribution assessment ($p < .05$).

	Reference							
	Fire	Harvesting	Non-stand replacing	Road	Total	User's accuracy	Producer's accuracy	Overall accuracy
Fire	0.444	0.003	0.006	0.000	0.453	0.98 ± 0.02	0.93 ± 0.04	0.92 ± 0.02
Harvesting	0.008	0.167	0.005	0.009	0.189	0.88 ± 0.05	0.88 ± 0.05	
Non-stand replacing	0.024	0.020	0.303	0.004	0.352	0.86 ± 0.07	0.96 ± 0.04	
Road	0.000	0.001	0.000	0.005	0.006	0.75 ± 0.07	0.36 ± 0.09	
Total	0.476	0.190	0.315	0.013	1.000			

but these gaps are rarely present in consecutive years due to the spatial randomness of cloud cover, compared to some systematic collection-related issue, such as SLC-off gaps. In addition to the absence of suitable observations, a considerable number of data gaps are flagged by filtering noisy observations, which are mostly caused by unscreened clouds, cloud shadows, haze, or smoke. This highlights the challenges and limitations not only of detecting clouds using a single date (Zhu and Woodcock 2012) but also the importance of time series for screening anomalous observations (Zhu and Woodcock 2014). When developing a protocol for implementation over large areas using thousands of images it is imperative that the data required for application of a given algorithm is systematically and consistently available. We initially aimed to include information related to the annual variability in spectral values within year, with difficulties arising due to a lack of consistency in image availability and subsequent valid pixels (cloud and shadow free) for the wider range of dates. Plus, the number of images that would be available to use to produce the within year variance information would vary, making the indicator inconsistent. As a result, we chose to produce a reliable annual rendition, using as much of the phenologically appropriate data as possible. Data blending (e.g. spatial / temporal fusion of MODIS and Landsat) does provide an opportunity for mitigating the variability in Landsat data yield within year and to enable systematic representation of a particular date(s) within year. For instance, Senf et al. (2015) demonstrate the application of synthetic Landsat data from data blending (after Hilker et al. 2009) in a land cover mapping context. Given the December 1999 launch of MODIS, applications combined with Landsat are largely only relevant post-2000 (e.g. Boschetti et al. 2015); given our earlier time series start date (1984) inclusion of such derived data was not deemed as applicable to our application.

The recent launch of the ESA's Sentinel-2 satellite (Drusch et al. 2012) will offer new opportunities to the image compositing field. Sentinel-2 has comparable spatial, spectral, and temporal characteristics with the Landsat sensor family, creating opportunities to combine the data from the satellites (Wulder, Hilker, et al. 2015). The calibrated measures made by Sentinel-2 will promote integration with those of Landsat. Integration of Landsat and Sentinel-2 data will allow for improved temporal revisit frequency, increasing the availability of observations free of atmospheric effects, thereby reducing the number of data gaps and their associated drawbacks in the image composites and change detection outcomes. With Landsat 7 and 8 combined with two Sentinel-2 instruments, there will be an opportunity for an image collected every 2–4 days, with the longer intervals occurring towards the equator (Wulder, Hilker, et al. 2015; Wulder, White, et al. 2015).

The implementation of the spectral trend analysis over wall-to-wall image composites permits the extension of temporal analyses from regional to national, continental, and even global scales (Griffiths, Müller et al. 2013; Hansen et al. 2013; Roy et al. 2015). Our change detection assessment results show the ability of spectral trend analysis of Landsat time series to accurately locate, delineate, and date stand-replacing and non-stand-replacing forest changes (Table 2). The spectral trend analysis of Landsat time series provides abundant information about forest changes that enables a rich description of disturbance aspects such as intensity, variability, or speed with which forest changes occur ultimately supporting the typing the change event with high accuracy (Table 4), especially for fire and harvesting events. The number of classes attributed to type in this implementation, while reflective of the dominant categories, are not exhaustive to the full range of change types present over Canada. The aim of the change hierarchy developed by Hermosilla et al. (2015b) is to acknowledge the categorical limitation, but to also provide framework for understanding what is mapped and to offer a means, given appropriate resources, to add further nested categorical detail. The Canada-wide assessment accuracies presented herein have high overall accuracy values for both change detection (89.0%) and change attribution (91.9%). The detection of fire and harvesting events is carried out with superior accuracy, being the roads the most challenging events to be correctly detected and attributed.

The level of the change categorization hierarchy selected was to be broadly inclusive of the main change types present over the forested area of Canada, especially the stand-replacing disturbances of wildfire and harvesting. The robustness of the random forest model, and related regional training

data collection strategy, combined with the spectral, spatial, and geometric distinctness of the change categories selected is illustrated in [Figure 6](#) with details of three Canadian ecozones dominated by different disturbance regimes presented. The Montane Cordillera case exhibits large areas of forest change, driven not only by the mid-2000s outbreak of the mountain pine beetle infestation but also by increases in logging activity in relation to this outbreak (Parkins and MacKendrick [2007](#)). Although geographically extensive, the insect infestation resulted in low rates of variation in the spectral response of the vegetation when compared to stand-replacing disturbances. The Taiga Shield West is an effective demonstration of the change dynamics in the unmanaged boreal forest, where the landscape is predominantly influenced by successive and widespread large fires (Stocks et al. [2002](#)). Finally, the Atlantic Maritime example shows the domination of harvesting activities as the main driver of forest change in southern coastal areas of eastern Canada (Power and Gillis [2001](#)). Not only are areas of change captured, but trends can also be described spatially, by jurisdiction or management status, or by other drivers supported by the relevant spatial datasets. Reporting on historical disturbance agents and trends, stratified by ecological or political units, establishes a foundation for future scientific applications as well as for meeting national and international reporting obligations.

The seamless Landsat surface reflectance image composites and the change events, characteristics, and types represent a single, nationally consistent and verifiable source of information with spatial (30 m) and temporal (annual) resolutions necessary to characterize natural and anthropogenic forest changes. The results presented here on amount and rate of stand-replacing and non-stand-replacing disturbance events support detailed national reporting of land cover dynamics, and enhance land management policies. The timely and spatially complete change products provide information well suited to improve the characterization of forest biomass over large areas and related modelling of carbon. Moreover, this unique data set facilitates previously not possible investigations of disturbance regimes at that national level over a range of disturbance agents, including and beyond wildfire and harvest. Additionally, due to the generation of detailed post-change spectral information and change metrics there is a refined ability to investigate how forests return following disturbance (Bartels et al. [2016](#)). Spectral information and metrics can be consulted to determine evidence of, and related rates, of forest regeneration (aka recovery) (Frazier, Coops, and Wulder [2015](#); Pickell et al. [2016](#)). As an additional application, the combination of the spectral information of the annual proxy composites, the change information, and the spectral trends can enable the development of annual land cover maps, making possible wall-to-wall quantification and mapping of forested land cover changes and land cover dynamics. The integration of the surface reflectance composite outcomes presented here with lidar data will be key for production of a national map of forest structure, including parameters such as canopy cover, biomass, and height (Pflugmacher, Cohen, and Kennedy [2012](#); Zald et al. [2016](#)).

The generated image composites cover the period 1984–2012 while the change characterization is focused on 1986–2010. With both programmes now considered operational, the imagery currently being collected by Landsat-8 OLI and Sentinel-2 are poised to support research and monitoring needs for the foreseeable future (Wulder, Hilker, et al. [2015](#)). Additionally, the recent advances in Landsat Multispectral Scanner data product development and custom processing techniques (Braaten et al. [2015](#)) indicate an increasing potential to further historically expand the time series of image composites and forest change products backwards until 1972 (Pflugmacher, Cohen, and Kennedy [2012](#)), while noting need for archival representation (Wulder, Hilker, et al. [2015](#)). The outcomes of this project can provide valuable baseline information from a consistent data source with the spatial and temporal resolution necessary to quantify and characterize natural and anthropogenic changes in forested ecosystems to support national monitoring programmes and a range of scientific applications within a Canadian context. Future NTEMS research is anticipated to focus on developing approaches to dynamically extend the temporal coverage of time series and forest change information as well as extending the attribute suite to include canopy cover, biomass, and height, as examples.

7. Conclusions

Availing upon the free and open analysis ready image data products made available via the USGS Landsat archive, novel and heretofore unavailable large area, time series characterizations are possible. In this work we comprehensively inform and enumerate on image inputs and data gaps that were addressed in the compositing process and enable a national assessment of our forest change detection and attribution techniques. Those interested in undertaking a project to characterize baseline conditions and subsequent trends are recommended to first undertake a metadata analysis of the Landsat archive contents. The metadata analysis will inform on the general amount as well as the spatial and temporal distribution of images available. The subsequent planning and methods development can then be linked to the expected archival image yield. Each stage of the data selection, composite rule application, through to subsequent composites and change products can be distinguished and quantified. Particularities of the quantification of each methodological stage provide insights into the quality and reliability of the information generated from the resultant composite and change products. The NTEMS was aimed to characterize the recent history of Canada's forests using the free and open access to analysis ready Landsat data. In this paper, we present outcomes produced through generating annual BAP composites and applying the C2C protocol to generate Canada-wide annual gap-free surface reflectance composites, and forest change and change type attribution layers. In so doing, we are able to accurately – temporally, spatially and by change type – report national summaries on the amount and rate of both stand-replacing (i.e. fire, harvesting, and roads) and non-stand-replacing change events. These outcomes provide baseline information on natural and anthropogenic changes in forested ecosystems to support national Canadian monitoring programmes and scientific applications. Our aim is that our communication enables clarity and transparency regarding our approach, but to also inform and assist others in implementation of similar projects.

ORCiD

Michael A. Wulder  <http://orcid.org/0000-0002-6942-1896>

Joanne C. White  <http://orcid.org/0000-0003-4674-0373>

Acknowledgments

This research was undertaken as part of the 'National Terrestrial Ecosystem Monitoring System (NTEMS): Timely and detailed national cross-sector monitoring for Canada' project jointly funded by the Canadian Space Agency (CSA), Government Related Initiatives Program (GRIP), and the Canadian Forest Service (CFS) of Natural Resources Canada.

Disclosure statement

No potential conflict of interest was reported by the authors.

References

- Banskota, A., N. Kayastha, M. J. Falkowski, M. A. Wulder, R. E. Froese, and J. C. White. 2014. "Forest Monitoring Using Landsat Time Series Data: A Review." *Canadian Journal of Remote Sensing* 40 (5): 362–384. [doi:10.1080/07038992.2014.987376](https://doi.org/10.1080/07038992.2014.987376).
- Bartels, S. F., H. Y. H. Chen, M. A. Wulder, and J. C. White. 2016. "Trends in Post-Disturbance Recovery Rates of Canada's Forests Following Wildfire and Harvest." *Forest Ecology and Management* 361: 194–207. [doi:10.1016/j.foreco.2015.11.015](https://doi.org/10.1016/j.foreco.2015.11.015).
- Boschetti, L., Roy, D. P., Justice, C. O., and Humber, M. L. 2015. "MODIS-Landsat Fusion for Large Area 30m Burned Area Mapping." *Remote Sensing of Environment* 161: 27–42. [doi:10.1016/j.rse.2015.01.022](https://doi.org/10.1016/j.rse.2015.01.022).
- Breiman, L. 2001. "Random Forests." *Machine Learning* 45 (1): 5–32. <http://www.springerlink.com/index/U0P06167N6173512.pdf>. doi:10.1023/A:1010933404324.

- Braaten, J. D., W. B. Cohen, and Z. Yang. 2015. "Automated Cloud and Cloud Shadow Identification in Landsat MSS Imagery for Temperate Ecosystems." *Remote Sensing of Environment* 169: 128–138. doi:10.1016/j.rse.2015.08.006.
- Canadian Forest Service. 2013. "Canada's National Forest Inventory, Revised 2006 Baseline." https://nfi.nfis.org/publications/standard_reports/NFI3_T4_FOR_AREA_en.html.
- Canadian Forest Service. 2015. "Canadian National Fire Database – Agency Fire Data." Natural Resources Canada, Canadian Forest Service, Northern Forestry Centre, Edmonton, Alberta. http://cwfis.cfs.nrcan.gc.ca/en_CA/nfdb.
- Cohen, W. B., Z. Yang, S. V. Stehman, T. A. Schroeder, D. M. Bell, J. G. Masek, C. Huang, and G. W. Meigs. 2016. "Forest Disturbance across the Conterminous United States from 1985–2012: The Emerging Dominance of Forest Decline." *Forest Ecology and Management* 360: 242–252. doi:10.1016/j.foreco.2015.10.042.
- Crist, E. 1985. "A TM Tasseled Cap Equivalent Transformation for Reflectance Factor Data." *Remote Sensing of Environment* 17: 301–306. doi:10.1016/0034-4257(85)90102-6.
- Drusch, M., U. Del Bello, S. Carlier, O. Colin, V. Fernandez, F. Gascon, B. Hoersch, et al. 2012. "Sentinel-2: ESA's Optical High-resolution Mission for GMES Operational Services." *Remote Sensing of Environment* 120: 25–36. doi:10.1016/j.rse.2011.11.026.
- Dymond, C. C., D. J. Mladenoff, and V. C. Radeloff. 2002. "Phenological Differences in Tasseled Cap Indices Improve Deciduous Forest Classification." *Remote Sensing of Environment* 80: 460–472. doi:10.1016/S0034-4257(01)00324-8.
- Ecological Stratification Working Group. 1995. "A National Ecological Framework for Canada." doi:Cat. No. A42-65/1996E; ISBN 0-662-24107-X.
- Frazier, R. J., N. C. Coops, and M. A. Wulder. 2015. "Boreal Shield Forest Disturbance and Recovery Trends Using Landsat Time Series." *Remote Sensing of Environment* 170: 317–327. doi:10.1016/j.rse.2015.09.015.
- Gómez, C., J. C. White, and M. A. Wulder. 2016. "Optical Remotely Sensed Time Series Data for Land Cover Classification: A Review." *ISPRS Journal of Photogrammetry and Remote Sensing* 116: 55–72. doi:10.1016/j.isprsjprs.2016.03.008.
- Gómez, C., J. C. White, and M. A. Wulder. 2011. "Characterizing the State and Processes of Change in a Dynamic Forest Environment Using Hierarchical Spatio-Temporal Segmentation." *Remote Sensing of Environment* 115 (7): 1665–1679. doi:10.1016/j.rse.2011.02.025.
- Goward, S. N., J. G. Masek, W. B. Cohen, G. G. Moisen, G. J. Collatz, S. P. Healey, R. A. Houghton, et al. 2008. "Forest Disturbance and North American Carbon Flux." *Eos, Transactions American Geophysical Union* 89 (11): 105–116.
- Griffiths, P., T. Kuemmerle, M. Baumann, V. C. Radeloff, I. V. Abrudan, J. Lieskovsky, C. Munteanu, K. Ostapowicz, and P. Hostert. 2013. "Forest Disturbances, Forest Recovery, and Changes in Forest Types across the Carpathian Ecoregion from 1985 to 2010 based on Landsat Image Composites." *Remote Sensing of Environment* 151. doi:10.1016/j.rse.2013.04.022.
- Griffiths, P., S. van der Linden, T. Kuemmerle, and P. Hostert. 2013. "A Pixel-Based Landsat Compositing Algorithm for Large Area Land Cover Mapping." *IEEE Journal of Selected Topics in Applied Earth Observations and Remote Sensing* 6 (5): 2088–2101.
- Griffiths, P., D. Müller, T. Kuemmerle, and P. Hostert. 2013. "Agricultural Land Change in the Carpathian Ecoregion after the Breakdown of Socialism and Expansion of the European Union." *Environmental Research Letters* 8 (4): 045024. doi:10.1088/1748-9326/8/4/045024.
- Hansen, M. C., and T. R. Loveland. 2012. "A Review of Large Area Monitoring of Land Cover Change Using Landsat Data." *Remote Sensing of Environment* 122: 66–74. doi:10.1016/j.rse.2011.08.024.
- Hansen, M. C., P. V. Potapov, R. Moore, M. Hancher, S. A. Turubanova, A. Tyukavina, D. Thau, et al. 2013. "High-resolution Global Maps of 21st-Century Forest Cover Change." *Science* (New York, N.Y.) 342 (6160): 850–853. doi:10.1126/science.1244693.
- Hermosilla, T., M. A. Wulder, J. C. White, N. C. Coops, and G. W. Hobart. 2015a. "An Integrated Landsat Time Series Protocol for Change Detection and Generation of Annual Gap-Free Surface Reflectance Composites." *Remote Sensing of Environment* 158: 220–234. doi:10.1016/j.rse.2014.11.005.
- Hermosilla, T., M. A. Wulder, J. C. White, N. C. Coops, and G. W. Hobart. 2015b. "Regional Detection, Characterization, and Attribution of Annual Forest Change from 1984 to 2012 Using Landsat-Derived Time-Series Metrics." *Remote Sensing of Environment* 170: 121–132. doi:10.1016/j.rse.2015.09.004.
- Hilker, T., Wulder, M. A., Coops, N. C., Seitz, N., White, J. C., Gao, F., Masek, J. G., and Stenhouse, G. 2009. "Generation of Dense Time Series Synthetic Landsat Data Through Data Blending with MODIS Using a Spatial and Temporal Adaptive Reflectance Fusion Model." *Remote Sensing of Environment* 113: 1988–1999.
- Ju, J., and J. G. Masek. 2016. "The Vegetation Greenness Trend in Canada and US Alaska from 1984–2012 Landsat Data." *Remote Sensing of Environment* 176: 1–16. doi:10.1016/j.rse.2016.01.001.
- Ju, J., and D. P. Roy. 2008. "The Availability of Cloud-Free Landsat ETM+ Data over the Conterminous United States and Globally." *Remote Sensing of Environment* 112 (3): 1196–1211. doi:10.1016/j.rse.2007.08.011.
- Kennedy, R. E., Z. Yang, and W. B. Cohen. 2010. "Detecting Trends in Forest Disturbance and Recovery Using Yearly Landsat Time Series: 1. LandTrendr – Temporal Segmentation Algorithms." *Remote Sensing of Environment* 114: 2897–2910. doi:10.1016/j.rse.2010.07.008.
- Kennedy, R. E., P. A. Townsend, J. E. Gross, W. B. Cohen, P. Bolstad, Y. Q. Wang, and P. Adams. 2009. "Remote Sensing Change Detection Tools for Natural Resource Managers: Understanding Concepts and Tradeoffs in the



- Design of Landscape Monitoring Projects." *Remote Sensing of Environment* 113 (7): 1382–1396. doi:10.1016/j.rse.2008.07.018.
- Keogh, E., S. Chu, D. Hart, and M. Pazzani. 2001. "An Online Algorithm for Segmenting Time Series." Proceedings IEEE International Conference on Data Mining, 2001. ICDM 2001. 289–296. doi:10.1109/ICDM.2001.989531.
- Key, C. H., and N. C. Benson. 2006. "Landscape Assessment (LA): Sampling and Analysis Methods." USDA Forest Service Gen. Tech. Rep. RMRS-GTR-164-CD.
- Kovalskyy, V., and D. P. Roy. 2013. "The Global Availability of Landsat 5 TM and Landsat 7 ETM+ Land Surface Observations and Implications for Global 30m Landsat Data Product Generation." *Remote Sensing of Environment* 130: 280–293. doi:10.1016/j.rse.2012.12.003.
- Lunetta, R. S., D. M. Johnson, J. G. Lyon, and J. Crotwell. 2004. "Impacts of Imagery Temporal Frequency on Land-Cover Change Detection Monitoring." *Remote Sensing of Environment* 89 (4): 444–454.
- Ma, Y., H. Wu, L. Wang, B. Huang, R. Ranjan, A. Zomaya, and W. Jie. 2015. "Remote Sensing Big Data Computing: Challenges and Opportunities." *Future Generation Computer Systems* 51 (2015): 47–60. doi:10.1016/j.future.2014.10.029.
- Markham, B. L., and D. L. Helder. 2012. "Forty-Year Calibrated Record of Earth-Reflected Radiance from Landsat: A Review." *Remote Sensing of Environment* 122 (2012): 30–40. doi:10.1016/j.rse.2011.06.026.
- Masek, J. G., E. F. Vermote, N. E. Saleous, R. Wolfe, F. G. Hall, K. F. Huemmrich, F. Gao, J. Kutler, and T. K. Lim. 2006. "A Landsat Surface Reflectance Dataset for North America, 1990–2000." *Geoscience and Remote Sensing Letters, IEEE* 3 (1): 68–72.
- McKenney, D. W., J. H. Pedlar, P. Papadopol, and M. F. Hutchinson. 2006. "The Development of 1901–2000 Historical Monthly Climate Models for Canada and the United States." *Agricultural and Forest Meteorology* 138 (1–4): 69–81. doi:10.1016/j.agrformet.2006.03.012.
- Mitchell, S. W., T. K. Remmel, F. Csillag, and M. A. Wulder. 2008. "Distance to Second Cluster as a Measure of Classification Confidence." *Remote Sensing of Environment* 112: 2615–2626. doi:10.1016/j.rse.2007.12.006.
- Olofsson, P., G. M. Foody, M. Herold, S. V. Stehman, C. E. Woodcock, and M. A. Wulder. 2014. "Good Practices for Estimating Area and Assessing Accuracy of Land Change." *Remote Sensing of Environment* 148: 42–57. doi:10.1016/j.rse.2014.02.015.
- Parkins, J. R., and N. A. MacKendrick. 2007. "Assessing Community Vulnerability: A Study of the Mountain Pine Beetle Outbreak in British Columbia, Canada." *Global Environmental Change* 17 (3–4): 460–471. doi:10.1016/j.gloenvcha.2007.01.003.
- Pflugmacher, D., W. B. Cohen, and R. E. Kennedy. 2012. "Using Landsat-Derived Disturbance History (1972–2010) to Predict Current Forest Structure." *Remote Sensing of Environment* 122: 146–165. doi:10.1016/j.rse.2011.09.025.
- Pickell, P. D., T. Hermosilla, R. J. Frazier, N. C. Coops, and M. A. Wulder. 2016. "Forest Recovery Trends Derived from Landsat Time Series for North American Boreal Forests." *International Journal of Remote Sensing* 37 (1): 138–149. doi:10.1080/2150704X.2015.1126375.
- Potapov, P. V., S. A. Turubanova, A. Tyukavina, A. M. Krylov, J. L. McCarty, V. C. Radeloff, and M. C. Hansen. 2015. "Eastern Europe's Forest Cover Dynamics from 1985 to 2012 Quantified from the Full Landsat Archive." *Remote Sensing of Environment* 159: 28–43. doi:10.1016/j.rse.2014.11.027.
- Power, K., and M. Gillis. 2001. "Canada's Forest Inventory 2001." Pacific Forestry Centre, 408. <http://www.cfs.nrcan.gc.ca/pubwarehouse/pdfs/26795.pdf>.
- Rogan, J., and D. Chen. 2004. "Remote Sensing Technology for Mapping and Monitoring Land-Cover and Land-use Change." *Progress and Planning* 61 (4): 301–325.
- Roy, D. P., J. Ju, K. Kline, P. L. Scaramuzza, V. Kovalskyy, M. Hansen, T. R. Loveland, E. Vermote, and C. Zhang. 2010. "Web-Enabled Landsat Data (WELD): Landsat ETM+ Composited Mosaics of the Conterminous United States." *Remote Sensing of Environment* 114 (1): 35–49. doi:10.1016/j.rse.2009.08.011.
- Roy, D. P., V. Kovalskyy, H. Zhang, and L. Yan. 2015. "The Utility of Landsat Data for Global Long Term Terrestrial Monitoring." In *Remote Sensing Time Series*, 22: 289–305. doi:10.1007/978-3-319-15967-6.
- Schmidt, G. L., C. B. Jenkerson, J. Masek, E. Vermote, and F. Gao. 2013. "Landsat Ecosystem Disturbance Adaptive Processing System (LEDAPS) Algorithm Description." <http://pubs.usgs.gov/of/2013/1057/>.
- Senf, C., P. J. Leitao, D. Pflugmacher, S. van der Linden, and P. Hostert. 2015. "Mapping Land Cover in Complex Mediterranean Landscapes using Landsat: Improved Classification Accuracies from Integrating Multi-Seasonal and Synthetic Imagery." *Remote Sensing of Environment* 156: 527–536. doi:10.1016/j.rse.2014.10.018.
- Sexton, J. O., X. P. Song, M. Feng, P. Noojipady, A. Anand, C. Huang, D. H. Kim, et al. 2013. "Global, 30-M Resolution Continuous Fields of Tree Cover: Landsat-based Rescaling of MODIS Vegetation Continuous Fields with Lidar-based Estimates of Error." *International Journal of Digital Earth* 6 (5): 427–448. doi:10.1080/17538947.2013.786146.
- Stocks, B. J., J. A. Mason, J. B. Todd, E. M. Bosch, B. M. Wotton, B. D. Amiro, M. D. Flannigan, et al. 2002. "Large Forest Fires in Canada, 1959–1997." *Journal of Geophysical Research* 108 (D1). doi:10.1029/2001JD000484.
- Townshend, J. R., J. Latham, C. O. Justice, A. Janetos, R. Conant, O. Arino, R. Balstad, et al. 2011. "Land Remote Sensing and Global Environmental Change." In *Remote Sensing and Digital Image Processing*, 11, edited by Bhaskar Ramachandran, Christopher O. Justice, and Michael J. Abrams, 835–856. New York, NY: Springer New York. doi:10.1007/978-1-4419-6749-7.

- Townshend, J. R., J. G. Masek, C. Huang, E. F. Vermote, F. Gao, S. Channan, J. O. Sexton, et al. 2012. "Global Characterization and Monitoring of Forest Cover Using Landsat Data: Opportunities and Challenges." *International Journal of Digital Earth* 5 (5): 373–397. doi:10.1080/17538947.2012.713190.
- Vogelmann, J. E., A. L. Gallant, H. Shi, and Z. Zhu. 2016. "Perspectives on Monitoring Gradual Change across the Continuity of Landsat Sensors Using Time-Series Data." *Remote Sensing of Environment*. doi:10.1016/j.rse.2016.02.060.
- White, J. C., and M. A. Wulder. 2013. "The Landsat Observation Record of Canada: 1972–2012." *Canadian Journal of Remote Sensing* 39 (6): 455–467. <http://www.tandfonline.com/doi/abs/10.1080/01431161.2013.779041>. doi:10.5589/m13-053.
- White, J. C., M. A. Wulder, G. W. Hobart, J. E. Luther, T. Hermosilla, P. Griffiths, N. C. Coops, et al. 2014. "Pixel-Based Image Compositing for Large-Area Dense Time Series Applications and Science." *Canadian Journal of Remote Sensing* 40 (3): 192–212. doi:10.1080/07038992.2014.945827.
- Woodcock, C. E., R. Allen, M. Anderson, A. Belward, R. Bindschadler, W. Cohen, F. Gao, et al. 2008. "Free Access to Landsat Imagery Teach by the Book Science Education." *Science* 320: 1011–10112. doi:10.1126/science.320.5879.1011a.
- Wulder, M. A., and N. C. Coops. 2014. "Make Earth Observations Open Access." *Nature* 513 (7516): 30–31. doi:10.1038/513030a.
- Wulder, M. A., T. Hilker, J. C. White, N. C. Coops, J. G. Masek, D. Pflugmacher, and Y. Crevier. 2015. "Virtual Constellations for Global Terrestrial Monitoring." *Remote Sensing of Environment* 170: 62–76. doi:10.1016/j.rse.2015.09.001.
- Wulder, M. A., W. A. Kurz, and M. Gillis. 2004. "National Level Forest Monitoring and Modeling in Canada." *Progress in Planning* 61 (4): 365–381. <http://www.citeulike.org/group/7954/article/4071276>.
- Wulder, M. A., J. G. Masek, W. B. Cohen, T. R. Loveland, and C. E. Woodcock. 2012. "Opening the Archive: How Free Data has Enabled the Science and Monitoring Promise of Landsat." *Remote Sensing of Environment* 122: 2–10. doi:10.1016/j.rse.2012.01.010.
- Wulder, M. A., J. C. White, M. M. Cranny, R. J. Hall, J. E. Luther, A. Beaudoin, D. G. Goodenough, and J. A. Dechka. 2008. "Monitoring Canada's Forests. Part 1: Completion of the EOSD Land Cover Project." *Canadian Journal of Remote Sensing* 34 (6): 549–562. doi:10.5589/m08-066.
- Wulder, M. A., J. C. White, T. R. Loveland, C. E. Woodcock, A. S. Belward, W. B. Cohen, E. A. Fosnight, J. Shaw, J. G. Masek, and D. P. Roy. 2015. "The Global Landsat Archive: Status, Consolidation, and Direction." *Remote Sensing of Environment*. doi:10.1016/j.rse.2015.11.032.
- Zald, H. S. J., M. A. Wulder, J. C. White, T. Hilker, T. Hermosilla, G. W. Hobart, and N. C. Coops. 2016. "Integrating Landsat Pixel Composites and Change Metrics with Lidar Plots to Predictively Map Forest Structure and Aboveground Biomass in Saskatchewan, Canada." *Remote Sensing of Environment* 176 (2016): 188–201. doi:10.1016/j.rse.2016.01.015.
- Zhou, L., C. J. Tucker, R. K. Kaufmann, D. Slayback, N. V. Shabanov, and R. B. Myneni. 2001. "Variations in Northern Vegetation Activity Inferred from Satellite Data of Vegetation Index during 1981 to 1999." *Journal of Geophysical Research* 106 (D17): 20069–20083. <http://onlinelibrary.wiley.com/doi/10.1029/2000JD000115/full>.
- Zhu, Z., and C. E. Woodcock. 2012. "Object-based Cloud and Cloud Shadow Detection in Landsat Imagery." *Remote Sensing of Environment* 118: 83–94. doi:10.1016/j.rse.2011.10.028.
- Zhu, Z., and C. E. Woodcock. 2014. "Automated Cloud, Cloud Shadow, and Snow Detection in Multitemporal Landsat Data: An Algorithm Designed Specifically for Monitoring Land Cover Change." *Remote Sensing of Environment* 152: 217–234. doi:10.1016/j.rse.2014.06.012.
- Zhu, Z., C. E. Woodcock, C. Holden, and Z. Yang. 2015. "Generating Synthetic Landsat Images based on All Available Landsat Data: Predicting Landsat Surface Reflectance at Any Given Time." *Remote Sensing of Environment* 162: 67–83. doi:10.1016/j.rse.2015.02.009.